J Physiol 588.9 (2010) pp 1489–1498

The Journal of Physiology

Characterisation of bipolar cell synaptic transmission in goldfish retina using paired recordings

Mary J. Palmer

Neuroscience Group, Institute for Science and Technology in Medicine, Keele University, Keele, UK

Direct recordings from the large axon terminals of goldfish retinal bipolar cells (BCs) have revealed detailed information about the properties and regulation of exocytosis at this ribbon-type synapse. However, the relationship between BC exocytosis and evoked postsynaptic responses in amacrine and ganglion cells is not known. To address this, I have made paired recordings from BC terminals (BCTs) and neurons in the ganglion cell layer (GCL) in goldfish retinal slices. BCT depolarisation evoked short-latency, AMPA/kainate receptor-mediated EPSCs in connected GCL neurons. NMDA receptors contributed to the response at +40 mV but not at −60 mV. Evoked EPSCs contained multiple temporal components that differed in their relative amplitudes between pairs. Changing the duration or amplitude of the presynaptic stimulus affected the size and kinetics of the EPSC, with weaker stimuli slowing the EPSC activation rate. Paired-pulse stimulation caused greater depression of fast than slow EPSC components. A linear relationship was found between the amount of BCT exocytosis, measured via changes in membrane capacitance, and the charge of evoked EPSCs, whether they were mediated by AMPA/kainate receptors alone or in combination with NMDA receptors. In addition, analysis of miniature EPSCs in GCL neurons provided estimates of the quantal content of evoked EPSCs. The results demonstrate the feasibility of using this paired recording system to study synaptic transfer at ribbon synapses, and indicate that both the rapid and sustained phases of BC exocytosis are encoded in the postsynaptic response.

(Received 9 December 2009; accepted after revision 8 March 2010; first published online 8 March 2010)
Corresponding author M. J. Palmer: Huxley Building, Keele University, Keele, Staffordshire ST5 5BG, UK. Email: m.j.palmer@cns.keele.ac.uk

Abbreviations BC, bipolar cell; BCT, bipolar cell terminal; C_m, membrane capacitance; GCL, ganglion cell layer; G_m, membrane conductance; G_s, series conductance; I_m, membrane current; IPL, inner plexiform layer; mEPSC, miniature EPSC; NBQX, 2,3-dioxo-6-nitro-1,2,3,4-tetrahydrobenzo[*f*]quinoxaline-7-sulfonamide; PPD, paired-pulse depression; RRP, rapidly releasable pool.

Introduction

Retinal bipolar cells (BCs) stimulate amacrine and ganglion cells by releasing glutamate at ribbon-type synapses, a specialisation of sensory neurons that signal via graded and sustained changes in membrane potential (Sterling & Matthews, 2005). Mb-type BCs from goldfish retina have been extensively used to study the exocytotic properties of ribbon synapses due to the accessibility of their large axon terminals for direct patch-clamp recording, which enables quantification of exocytosis via changes in membrane capacitance (C_m). BC terminal (BCT) depolarisations that maximally activate Ca^{2+} influx evoke a very rapid phase of exocytosis of limited capacity followed by a slower, more sustained phase (Mennerick & Matthews, 1996). These phases are believed to correspond with the release of synaptic vesicles docked at the base of ribbons (the rapidly releasable pool, RRP) and those tethered higher up the ribbon (the reserve pool), respectively (von Gersdorff *et al.* 1996). Two components of exocytosis are also observed in responses evoked by glutamate release from isolated BCTs, using horizontal cells as a reporter system (Sakaba *et al.* 1997; von Gersdorff *et al.* 1998).

The amacrine/ganglion cell response to the transient and sustained phases of BC exocytosis will depend on the subtypes and activation properties of postsynaptic glutamate receptors. AMPA and kainate receptors normally desensitise rapidly to glutamate, which may preclude them from detecting sustained exocytosis and contribute to the conversion from sustained to transient signalling at BC synapses (Lukasiewicz *et al.* 1995;

DOI: 10.1113/jphysiol.2009.185850

Maguire, 1999). The effects of AMPA/kainate receptor desensitisation may be negated by the expression of NMDA receptors, which appear to be required for detecting sustained exocytosis at BC synapses in newt retina (Matsui *et al.* 1998). By contrast, evoked EPSCs mediated by Ca^{2+}-permeable AMPA receptors at the rod BC to AII amacrine cell synapse in rat retina appear to be less susceptible to desensitisation. EPSC time-course is mainly determined by release kinetics rather than receptor desensitisation, with weaker or slower BC depolarisations evoking more sustained responses (Singer & Diamond, 2003; Snellman *et al.* 2009). However, the quantitative relationship between BC exocytosis and evoked postsynaptic responses remains unknown. Here, I exploit the ability to record directly from BCTs in goldfish retinal slices (Palmer *et al.* 2003) to address this issue by making paired recordings from BCTs and synaptically connected neurons in the ganglion cell layer (GCL). The results indicate that postsynaptic responses accurately signal both the rapid and sustained phases of exocytosis at this synapse.

Methods

Goldfish (*Carassius auratus*) were dark-adapted for 1 h and killed by decapitation followed immediately by destruction of the brain and spinal cord under Schedule 1 of the UK Animals (Scientific Procedures) Act 1986. The experiments conformed with guidelines laid down by the animal welfare committee of Keele University, and comply with *The Journal of Physiology*'s policies on animal experimentation (Drummond, 2009). The eyeballs were removed and retinae dissected out and treated for 25 min with hyaluronidase to remove vitreous humor. Each retina was quartered, placed ganglion cell layer down on filter paper and kept at 4°C in medium comprising (mM): NaCl 127, KCl 2.5, $MgCl_2$ 1.0, $CaCl_2$ 0.5, Hepes 5 and glucose 12, adjusted to pH 7.45 with NaOH.

Slices were cut at 250 μm intervals, transferred to the recording chamber and perfused ($\sim$1 ml min^{-1}) with medium comprising (mM): NaCl 108, KCl 2.5, $MgCl_2$ 1.0, $CaCl_2$ 2.5, $NaHCO_3$ 24 and glucose 12, gassed with 95% O_2–5% CO_2, pH 7.4. Slice preparation and recordings were performed at room temperature, in daylight conditions. Patch-pipettes (5–8 MΩ) were pulled from borosilicate glass and coated in dental wax. Intracellular solutions comprised (mM): caesium-methane-sulphonate 115, Hepes 25, TEA-Cl 10, Mg-ATP 3, Na-GTP 0.5 and EGTA 0.5, pH 7.2; and: potassium-methane-sulphonate or potassium gluconate 110, Hepes 25, KCl 10, $MgCl_2$ 5, Mg-ATP 3, Na-GTP 0.5 and EGTA 0.5, pH 7.2. Cs^+-based intracellular solution was used for all GCL neuron recordings; Cs^+- or K^+-based solution was used for BCT recordings. No differences in the properties of evoked EPSCs were observed between solutions. The intracellular solution also normally contained the fluorescent dye Lucifer Yellow (0.5 mg ml^{-1}).

Simultaneous whole-cell voltage-clamp recordings were obtained from visually identified GCL neurons and large axon terminals of mixed-input BCs in the inner plexiform layer (IPL; Fig. 1*A*). The distance between recorded neurons ranged from a few micrometers to approximately 30 μm, but was normally less than 10 μm. BCT recordings were made from both intact BCs and axon-severed terminals (determined by their capacitive current, Palmer *et al.* 2003). No differences in evoked EPSCs were observed between axon-severed and intact BCT recordings. The electrophysiological properties of GCL neurons were determined from their response to depolarising voltage steps, which evoked transient inward currents in 82 of 137 recordings. However, in the majority of synaptically connected recordings (32 of the 35 analysed pairs), the GCL neuron lacked voltage-activated inward currents and exhibited a characteristic outwardly rectifying *I–V* relationship. These GCL neurons, which may be displaced amacrine cells (Yazulla *et al.* 1986), were relatively small in size (7.8 ± 0.4 pF, $n = 32$, compared with 11.4 ± 0.7 pF, $n = 65$, for unconnected GCL neurons, $P < 0.01$) and were normally located near the GCL–IPL border. The size and kinetics of recorded EPSCs are susceptible to errors resulting from poor space-clamp, particularly in large neurons with complex morphologies (Williams & Mitchell, 2008). These errors are likely to be minimised by the small size of the connected GCL neurons and the short distance between presynaptic and postsynaptic recordings. In addition, the small amplitude of evoked EPSCs and lack of voltage-gated Na^+ currents will reduce the likelihood of escape from voltage-clamp during EPSCs at sites of synaptic input.

Drugs were bath-applied via the extracellular solution. The $GABA_{A/C}$ receptor antagonist picrotoxin (50 μM) and the glycine receptor antagonist strychnine (1 μM) were present in approximately half the recordings, including all recordings in which the GCL neuron was held at +40 mV, to eliminate inhibitory synaptic currents. Picrotoxin and strychnine had no effect on the size or kinetics of evoked responses at −60 mV. Picrotoxin, 2,3-dioxo-6-nitro-1,2,3,4-tetrahydrobenzo[*f*]quinoxaline-7-sulfonamide (NBQX), and D-(−)-2-amino-5-phosphonopentanoic acid (D-AP5) were obtained from Tocris (Bristol, UK); other salts and chemicals were obtained from Sigma-Aldrich (Gillingham, UK) or Fisher Scientific (Loughborough, UK).

An EPC-10 double patch-clamp amplifier with Patchmaster software (HEKA, Lambrecht/Pfalz, Germany) was used to control membrane voltage (V_m) and record membrane current (I_m) in BCTs and GCL neurons. Series resistance (R_s) in the analysed paired recordings was 23 ± 1 MΩ (range 11–35 MΩ)

for the BCTs and 32 ± 2 MΩ (range 17–68 MΩ) for the GCL neurons ($n = 35$), and was uncompensated. C_m measurements of exocytosis in axon-severed BCTs were performed using the 'sine + DC' method. In brief, a 1 kHz sinusoidal voltage command (30 mV peak-to-peak) was added to the holding potential of −60 mV and the resulting I_m analysed at two orthogonal phase angles by the EPC-10 software emulation of a lock-in amplifier. These signals, together with the DC current, were used to generate values for C_m, membrane conductance (G_m) and series conductance (G_s). C_m measurements were used for analysis only if there were no accompanying changes in G_m or G_s.

During paired recordings, BCTs were depolarised at 20 s intervals and each stimulus was delivered multiple times to enable average EPSCs to be calculated and reduce the influence of spontaneous current fluctuations on EPSC charge measurements. As evoked EPSCs tended to run-down during recordings due to run-down of BCT exocytosis (Palmer *et al.* 2003), both C_m increases and the size of EPSCs evoked by different stimuli were measured during the initial recording period using interleaved stimuli. The amount of EPSC run-down during this period is shown in Fig. 1*G* ($n = 16$). Recordings exhibiting >50% run-down were not used for analysis.

Off-line analysis was performed using IgorPro software (WaveMetrics, Lake Oswego, OR, USA). EPSC latency was measured as the time interval between the start of the BCT depolarisation and the initial point of rise of the EPSC, determined by eye. EPSC charge was measured as the integral of baseline-subtracted I_m traces, and EPSC activation rate was measured as the rate of rise of the first EPSC component. Spontaneous and evoked miniature EPSCs (mEPSCs) were identified by their rate of rise and analysed using custom software kindly provided by Dr H. Taschenberger. Evoked mEPSCs were classified as events that occurred within 500 ms of stimulation and were analysed in GCL neurons exhibiting low frequencies (<0.1 Hz) of spontaneous mEPSCs. In neurons exhibiting higher frequencies of spontaneous mEPSCs, recording periods without stimulation were used for analysis. Pooled data are expressed as mean ± S.E.M.; statistical significance was assessed using Student's *t* tests, with $P < 0.05$ considered significant.

Results

Paired voltage-clamp recordings were made from BCTs and GCL neurons in goldfish retinal slices, with both neurons held at −60 mV. BCT depolarisation to −10 mV for 25 ms, a stimulus that releases the RRP (Mennerick & Matthews, 1996), evoked an EPSC in the GCL neuron in 54 of 137 paired recordings (Fig. 1*B*). Of these, 38 were of sufficient quality in terms of recording length, signal-to-noise ratio and stability of responses to permit subsequent analysis of evoked EPSCs. The EPSC exhibited a long latency (6.8–7.8 ms) in three recordings, which were not analysed further. In the remaining recordings, EPSC latency ranged from 0.8 ms to 3.1 ms (mean 1.5 ± 0.1 ms, $n = 35$). Evoked EPSCs contained multiple temporal components. The first component peaked within 4 ms of stimulation and was defined as the rapid EPSC component (mean peak latency $= 2.8 \pm 0.1$ ms, $n = 26$). The rapid component was normally followed by one or more slower components that prolonged the EPSC duration to up to 120 ms. The occurrence and relative amplitudes of the EPSC components showed little inter-trial variability within pairs but differed markedly between pairs (Fig. 1*B–E*). EPSC amplitude ranged from −4 pA to −60 pA. Application of the AMPA/kainate receptor antagonist NBQX (5–10 μM) abolished all components of the evoked EPSC at −60 mV ($n = 4$; Fig. 1*C* and *E*). The NMDA receptor antagonist D-AP5 (50–100 μM) was applied to two recordings in which the EPSC had a prominent slow component, but had no effect on the kinetics of the response.

BCT depolarisations were also delivered with the GCL neuron held at +40 mV to relieve the voltage-dependent block of NMDA receptors. EPSCs evoked at +40 mV had slow kinetics and carried more charge than at −60 mV (EPSC charge ratio (+40 mV/−60 mV) $= 5.0 \pm 1.4$, $n = 10$). The additional slow EPSC component evoked at +40 mV was inhibited by D-AP5 (100 μM; $n = 2$; Fig. 1*D*). Slow evoked EPSCs at +40 mV were also observed following inhibition of the response at −60 mV with NBQX (5 μM; Fig. 1*E*). Further evidence for the lack of NMDA receptor activation at −60 mV was obtained from a subset of paired recordings (5 of 26) that showed no evoked EPSC at −60 mV but a slow D-AP5-sensitive response at +40 mV, suggesting an NMDA receptor-only synaptic connection (Fig. 1*F*).

Depolarisation of BCTs evokes a rapid phase of exocytosis followed by slower but more sustained release (Mennerick & Matthews, 1996). For depolarisations to −10 mV, the rapid phase occurs with a time-constant of ∼0.8 ms (Fig. 2*A*). The effect of stimulus duration on the size and kinetics of evoked EPSCs was therefore investigated. With the GCL neuron held at −60 mV, reducing the stimulus duration from 25 ms to 1 ms (at −10 mV) had little effect on the rapid component of the EPSC but decreased the amplitude and duration of the slower components (Fig. 2*B*). Increasing the stimulus duration from 25 ms to 200 ms (at −10 mV) normally increased the duration of the evoked EPSC (Fig. 2*C*). Changing the stimulus duration with the GCL neuron held at +40 mV had similar effects on the amplitude and duration of evoked responses (Fig. 2*B* and *C*).

BCT depolarisation to the more physiologically relevant potential of −30 mV evokes less exocytosis than

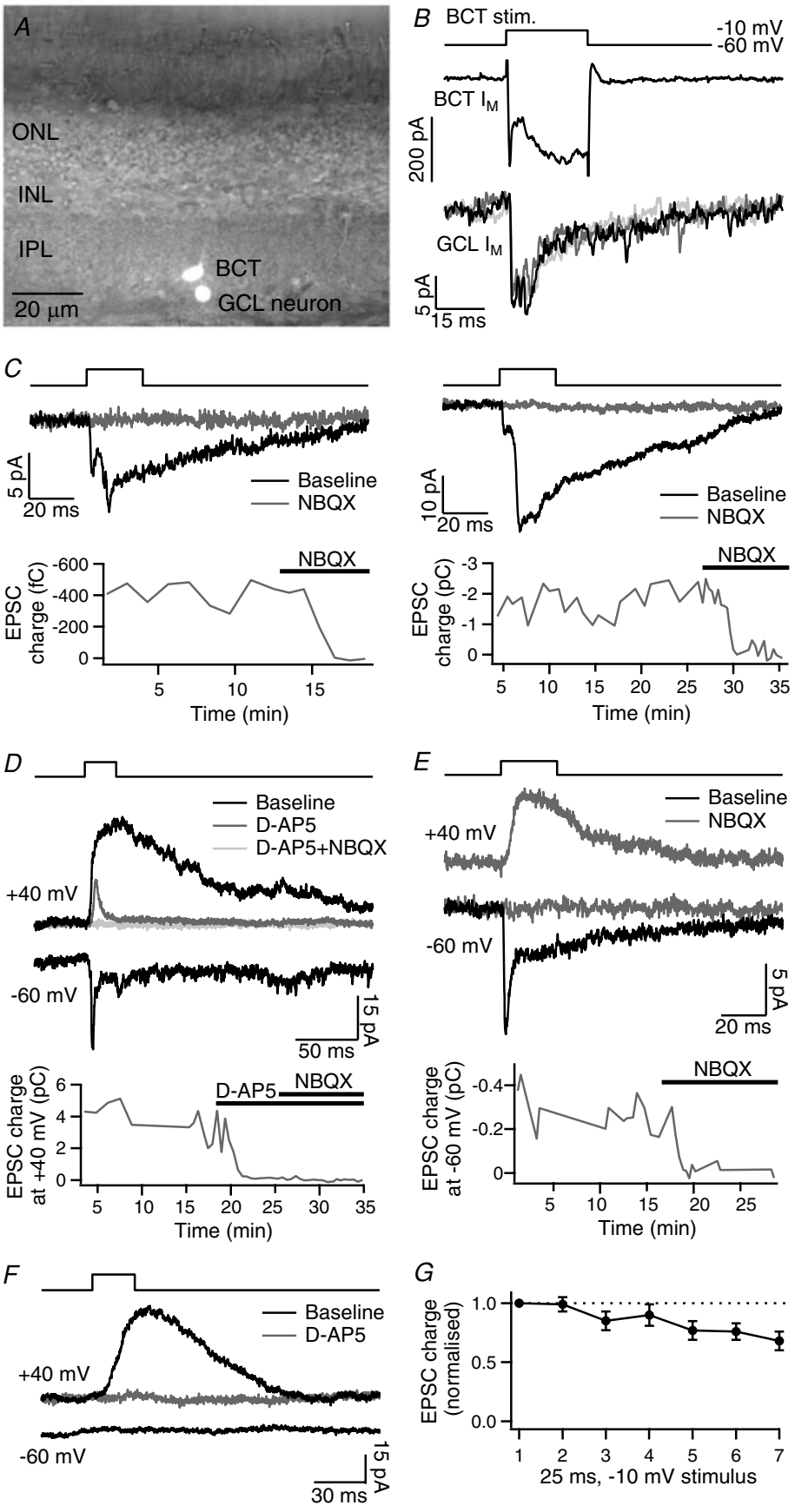

depolarisation to −10 mV, with the rapid phase occurring at a slower rate (time-constant ∼9.4 ms; Fig. 2*A*), due to the voltage dependence of Ca^{2+} channel activation and the Ca^{2+} dependence of release (Heidelberger *et al.* 1994; Mennerick & Matthews, 1996; Mennerick & Matthews, 1998; Burrone & Lagnado, 2000). To investigate the effect of stimulus amplitude on evoked EPSCs, BCT depolarisations were reduced from −10 mV to −30 mV (for 25 ms). With the GCL neuron held at −60 mV, EPSCs evoked by depolarisation to −30 mV had a smaller amplitude, a longer latency and/or a slower activation rate than EPSCs evoked by −10 mV depolarisations (Fig. 2*D* and *E*). Similar effects were observed with the GCL neuron held at +40 mV (Fig. 2*D*).

BCTs exhibit pronounced paired-pulse depression (PPD) of exocytosis that is likely to reflect depletion of releasable vesicles and requires at least 10 s for full recovery (Mennerick & Matthews, 1996; von Gersdorff & Matthews, 1997). For the C_m increase evoked by a pair of 25 ms, −10 mV depolarisations (100 ms interval), PPD (p2/p1) = 0.24 ± 0.01 (n = 94; Fig. 3*A*). To analyse the time-course of exocytosis during these paired stimuli, −10 mV depolarisations of varying duration (1, 5, 10, 25 ms) were delivered alone or 100 ms after a 25 ms, −10 mV depolarisation (Fig. 3*B*). The rapid phase of exocytosis was found to be more strongly depressed than the sustained phase during p2. The effect of PPD on evoked EPSCs was investigated by delivering paired 25 ms, −10 mV depolarisations (100 ms interval) with the GCL neuron held at −60 mV. In response to p2, the faster components of the EPSC were strongly depressed (rapid component: p1 = −9.5 ± 1.1 pA, p2 = −1.6 ± 0.3 pA, PPD = 0.19 ± 0.04, n = 9; Fig. 3*C* and *D*). However, when the evoked EPSC contained a prominent slow component, this component showed little depression (EPSC measured at 40–60 ms: p1 = −17 ± 5 pA, p2 = −13 ± 3 pA, PPD = 0.87 ± 0.12, n = 6; Fig. 3*D*). The amount of PPD of the evoked response therefore varied considerably between recordings (PPD of EPSC charge = 0–0.89), depending on EPSC kinetics.

In order to determine whether evoked EPSCs accurately signal the amount of glutamate release from BCTs, the charge of EPSCs evoked at −60 mV and +40 mV was compared with C_m measurements of exocytosis. As the BCT in 18 of the 35 analysed paired recordings was not an axon-severed terminal (i.e. remained attached to the BC soma, a configuration that provides less reliable C_m measurements), the charge of EPSCs evoked by different stimuli was compared with the C_m increase evoked by the same stimuli measured in a large set of axon-severed BCT recordings (n = 45–94). The C_m increase and the EPSC charge for each stimulus were normalised to that evoked by a 25 ms, −10 mV depolarisation in the same BCT or paired recording. The charge of EPSCs evoked at −60 mV by stimulus durations of 1 ms (n = 19) and 200 ms (n = 14), a stimulus amplitude of −30 mV (n = 15), and by paired stimuli (n = 23) were compared with that evoked by a 25 ms, −10 mV stimulus. For EPSCs evoked at +40 mV, EPSC charge evoked by stimulus durations of 1 ms (n = 4) and 200 ms (n = 7), and a stimulus amplitude of −30 mV (n = 7) were compared with that evoked by a 25 ms, −10 mV stimulus. EPSC charge was found to be linearly related to the amount of BC exocytosis for all stimulus conditions tested, for responses evoked at −60 mV (Fig. 4*A*) and at +40 mV (Fig. 4*B*).

In some GCL neurons, mEPSCs were observed during the tail of evoked responses (n = 4; Fig. 5*A*), or occurring spontaneously at low frequencies (1.2 ± 0.3 Hz, n = 9). Average evoked and spontaneous mEPSCs at −60 mV had rapid kinetics with a bi-exponential decay (10–90% rise-time = 0.30 ± 0.02 ms, decay τ_1 = 0.76 ± 0.03 ms, accounting for 89 ± 1% of the decay, τ_2 = 16 ± 3 ms, n = 13; Fig. 5*B*), an average amplitude of −7.1 ± 0.4 pA (n = 13) and were eliminated by the AMPA/kainate receptor antagonist NBQX (5 μM, n = 2). Amplitude histograms of mEPSCs showed a fairly symmetrical

Figure 1. Paired recordings of evoked EPSCs
A, light microscope image of a synaptically connected bipolar cell terminal (BCT) and neuron in the ganglion cell layer (GCL), filled with Lucifer Yellow, in a goldfish retinal slice (IPL, inner plexiform layer; INL, inner nuclear layer; ONL, outer nuclear layer). *B*, membrane current (I_m) responses in a BCT (Cs^+-based intracellular solution) and a connected GCL neuron to 25 ms depolarisations from −60 mV to −10 mV. Three example GCL neuron responses are shown overlaid. In subsequent figures, GCL neuron I_m traces show averages of between 3 and 10 EPSCs in each pair. *C*, EPSCs evoked by the same stimulus showing the variability between pairs in the relative amplitudes of the EPSC components, and the block of EPSCs by the AMPA/kainate receptor antagonist NBQX (5–10 μM). *D*, evoked EPSCs with the GCL neuron held at −60 mV and +40 mV. Addition of the NMDA receptor antagonist D-AP5 (100 μM) inhibited the large slow component at +40 mV; subsequent addition of NBQX (10 μM) inhibited the remaining fast component. *E*, following inhibition of evoked EPSCs at −60 mV with NBQX (5 μM), slow EPSCs remained at +40 mV. *F*, an example recording that showed no evoked response at −60 mV but a large response at +40 mV, which was eliminated by D-AP5 (100 μM). *G*, average charge of EPSCs evoked by 25 ms, −10 mV depolarisations during the recording period used for comparison of different stimuli, to show the amount of run-down (n = 16).

distribution and an absence of large events (Fig. 5*C*). As the amplitude of evoked asynchronous mEPSCs was similar to that of spontaneous mEPSCs (Fig. 5*D*), the evoked events are likely to be uniquantal (Singer *et al.* 2004). The relative charge of average mEPSCs and evoked EPSCs was used to estimate the quantal content of responses evoked by a 25 ms, −10 mV stimulus in 11 paired recordings. This analysis relies on various assumptions, primarily that the recorded mEPSCs are representative of quantal events at the activated BCT to GCL neuron synapse, and that the evoked EPSC consists of a linear summation of mEPSCs. In support of

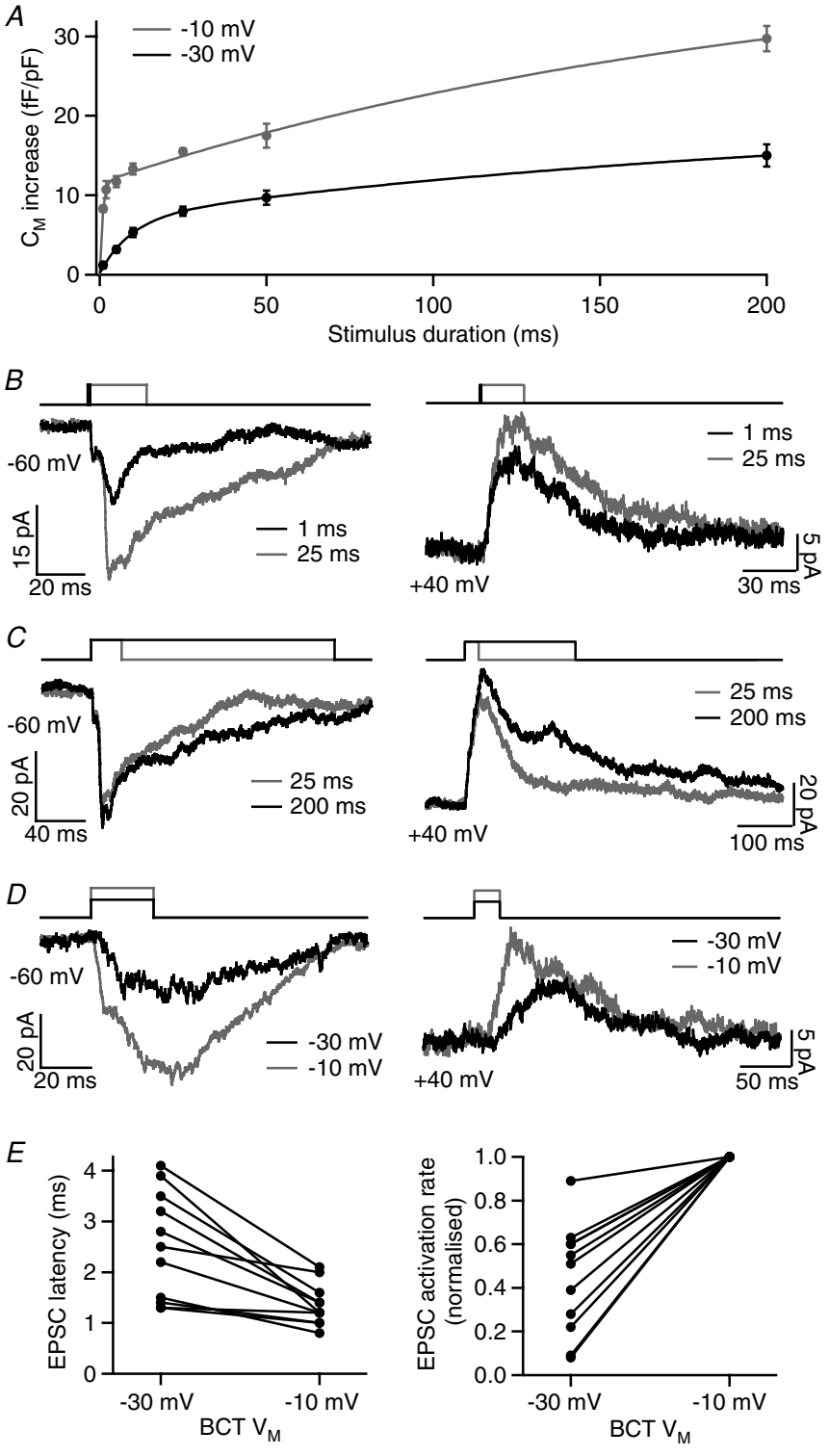

Figure 2. The effect of BCT stimulus duration and amplitude on evoked EPSCs
A, the rate of BCT exocytosis during depolarisation to −10 and −30 mV, as measured by the C_m increase evoked by step depolarisations of between 1 and 200 ms duration in axon-severed BCTs. Both sets of data were fitted with a double-exponential function (−10 mV: $\tau_1 = 0.83$ ms, $\tau_2 = 201$ ms; −30 mV: $\tau_1 = 9.4$ ms, $\tau_2 = 229$ ms; $n = 7$–34). *B*, example EPSCs showing the effect of decreasing the stimulus duration from 25 ms to 1 ms (−10 mV steps), with the GCL neuron held at −60 or +40 mV. *C*, example EPSCs showing the effect of increasing the stimulus duration from 25 ms to 200 ms (−10 mV steps), with the GCL neuron held at −60 or +40 mV. *D*, example EPSCs showing the effect of decreasing the BCT depolarisation from −10 mV to −30 mV (25 ms duration), with the GCL neuron held at −60 or +40 mV. *E*, EPSC latency and activation rate (GCL neuron at −60 mV) for EPSCs evoked by BCT depolarisations to −30 and −10 mV in 11 paired recordings (EPSC activation rate is shown normalised to the −10 mV value due to the large variation between pairs).

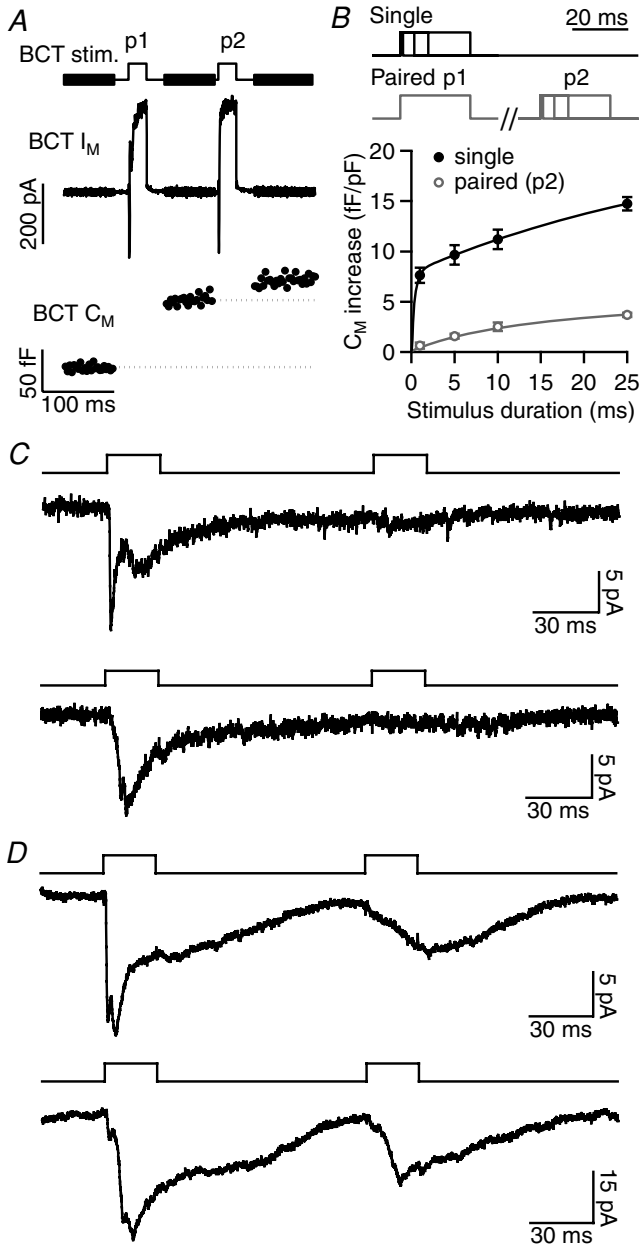

Figure 3. The effect of paired-pulse depression (PPD) of exocytosis on evoked EPSCs
A, example I_m and C_m responses in an axon-severed BCT (K^+-based intracellular solution) to a pair of 25 ms depolarisations to −10 mV (100 ms interval), shown above. BCT exocytosis exhibits PPD. *B*, the stimulus protocols (top) and average C_m increase (below) evoked by −10 mV depolarisations of varying duration delivered alone (single) or 100 ms after a 25 ms, −10 mV depolarisation (paired; $n = 7$–27). The initial rapid phase of exocytosis was not observed during p2. *C*, EPSCs evoked by paired 25 ms, −10 mV stimuli in two example recordings in which the EPSC showed strong PPD. *D*, EPSCs evoked by paired 25 ms, −10 mV stimuli in two example recordings that exhibited less PPD. In these recordings, the p2 EPSC resembled the slow component of the p1 EPSC.

the second assumption, the linear relationship between exocytosis and EPSC charge suggests that receptor saturation and desensitisation are limited, and that glutamate clearance is fairly rapid, at this synapse. In nine pairs in which the evoked EPSC exhibited fairly rapid

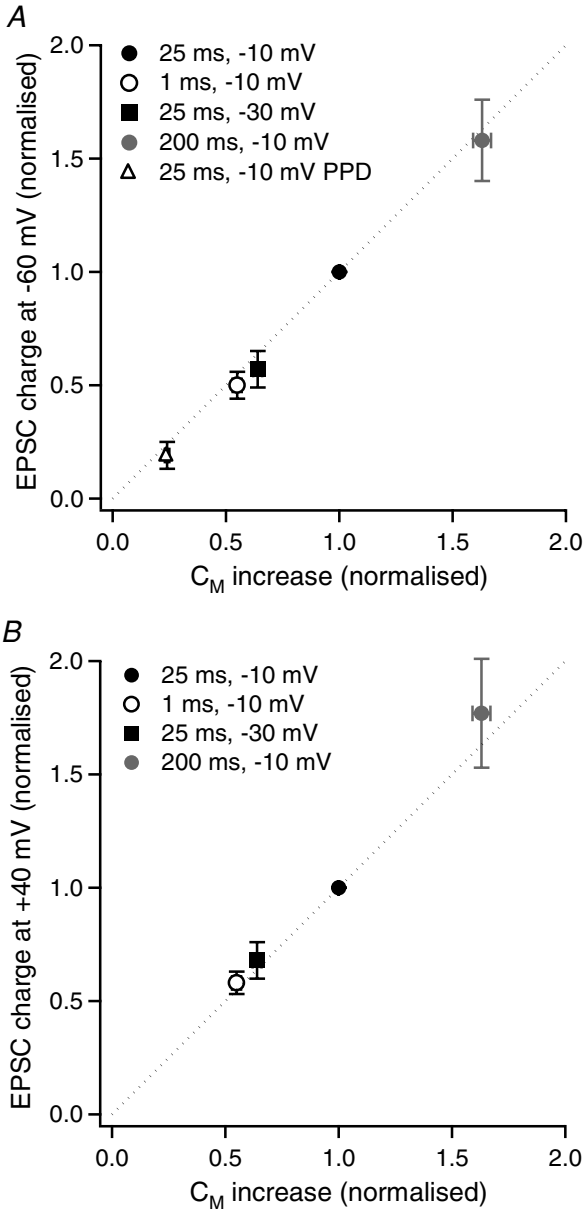

Figure 4. The relationship between BCT exocytosis and EPSC charge
A, mean charge of EPSCs mediated by AMPA/kainate receptors at −60 mV evoked by a range of stimuli, normalised to the charge of EPSCs evoked by a 25 ms, −10 mV stimulus in the same paired recording ($n = 14$–23) *versus* mean C_m increase, normalised to the C_m increase evoked by a 25 ms, −10 mV stimulus, in axon-severed BCTs ($n = 45$–94). The dashed line shows a 1:1 ratio. *B*, as for *A*, but for EPSCs mediated by AMPA/kainate and NMDA receptors at +40 mV ($n = 4$–7 for EPSC charge values).

kinetics, the estimated quantal content ranged from 9 to 40 (mean = 23 ± 4; Fig. 5*E* and *F*). In the remaining two pairs, the EPSC contained a prominent slow component, and the estimated quantal content was substantially higher (106 and 333; Fig. 5*F*).

Discussion

Paired recordings enable precise control of presynaptic activity together with measurement of both neurotransmitter release and the evoked postsynaptic response, thus providing detailed information about the properties of transmission at individual synapses. Here I extend the limited range of synapses that can be studied with paired recordings to include the large-terminal BCs of goldfish retina, which are used as a model system for studying the properties of ribbon synapses (Sterling & Matthews, 2005). I describe the properties of EPSCs evoked by stimuli of varying amplitude and duration (1–200 ms) in connected GCL neurons, and show that the postsynaptic response accurately reflects the amount of BCT exocytosis.

EPSCs evoked in GCL neurons by BCT depolarisation to −10 mV had a short latency (∼1.5 ms) and were blocked by AMPA/kainate and NMDA receptor antagonists,

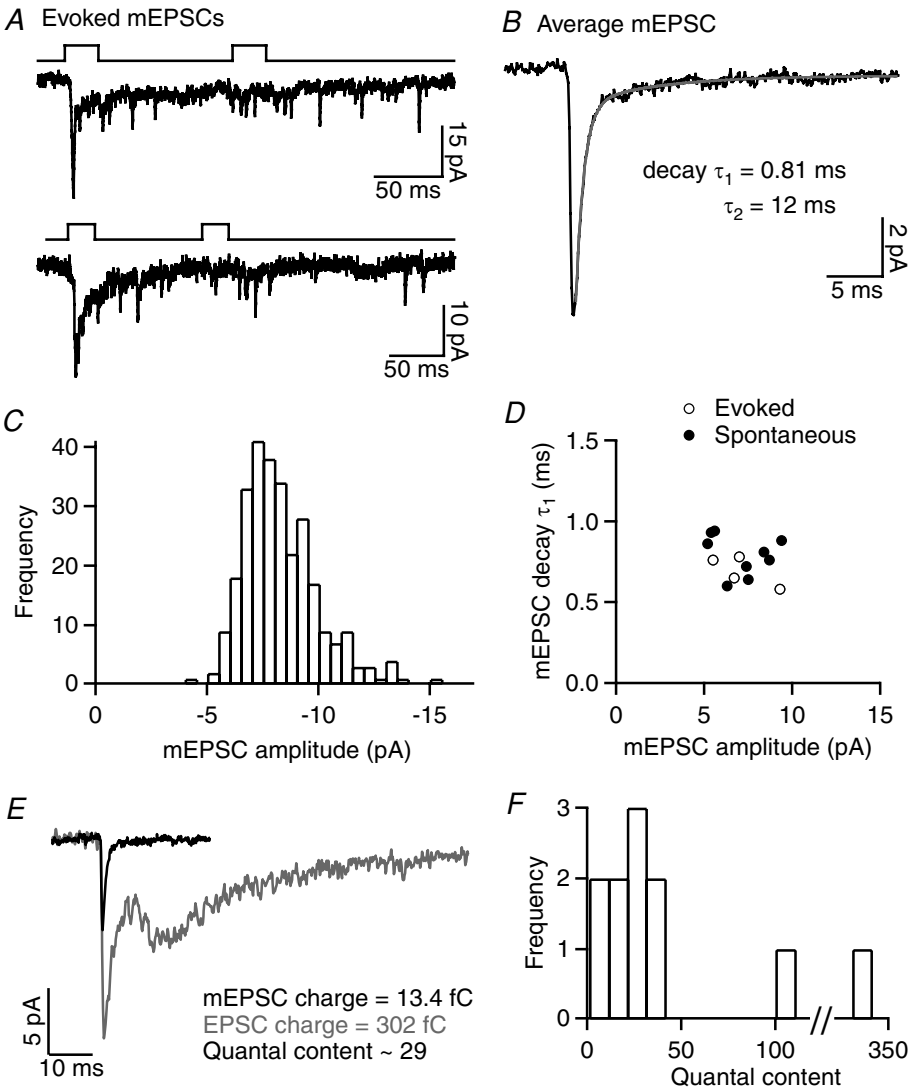

Figure 5. Estimation of the quantal content of evoked EPSCs
A, individual EPSCs evoked by paired 25 ms, −10 mV stimuli in two GCL neuron recordings in which mEPSCs were observed during the tail of the response. *B*, the average mEPSC in a GCL neuron that exhibited spontaneous mEPSCs, with the time-constants for a double-exponential fit of the mEPSC decay. *C*, the mEPSC amplitude histogram from another GCL neuron that exhibited spontaneous mEPSCs. *D*, properties of average evoked or spontaneous mEPSCs recorded in 13 GCL neurons. *E*, example recording in which the relative charge of the average mEPSC and evoked EPSC (shown superimposed) was used to estimate quantal content. *F*, histogram showing the estimated quantal content of EPSCs evoked by a 25 ms, −10 mV stimulus in 11 paired recordings.

consistent with a monosynaptic glutamatergic connection. Most of the synaptic delay can be accounted for by the rate of Ca^{2+} channel activation ($\tau \sim 0.6$ ms, Mennerick & Matthews, 1998) and the delay between Ca^{2+} influx and exocytosis (~0.5 ms, Heidelberger *et al.* 1994). Reducing BCT depolarisation to a more physiologically relevant potential (−30 mV) increased the latency and slowed the rise-time of evoked EPSCs, effects that were also observed using isolated BCTs (von Gersdorff *et al.* 1998) and at the rod BC to AII synapse (Singer & Diamond, 2003). Postsynaptic responses evoked by small, physiological stimuli are therefore likely to have a slow activation rate. In addition, the amplitude and duration of evoked EPSCs were dependent on the amplitude and duration of BCT depolarisations, suggesting that GCL neuron responses are able to reflect the graded and sustained changes in BC V_m that occur during light responses.

Evoked EPSCs were small in comparison with EPSCs at rod BC to AII synapses, which can have a peak amplitude of several hundred picoamps, but were similar in size to EPSCs at rod BC to A17 synapses (~12 pA, Singer & Diamond, 2003; Veruki *et al.* 2003). The large size of EPSCs evoked in AII cells results from both a larger quantal amplitude and multiple (7–12) release sites per synaptic connection (Singer *et al.* 2004). Comparison of the estimated quantal content of EPSCs evoked by a stimulus that releases the RRP (9–40) with the reported number of docked vesicles at goldfish BC synaptic ribbons (16–22, von Gersdorff *et al.* 1996; Llobet *et al.* 2003) suggests that the synaptic connection studied here comprises only one or two release sites. The distinct temporal components of the evoked EPSC may arise from the heterogeneous release probabilities of vesicles within the RRP, which result from their varying distances from Ca^{2+} channels (Burrone *et al.* 2002; Beaumont *et al.* 2005).

In some recordings the evoked EPSC contained a particularly large slow component. An analogous delayed component evoked by glutamate release from isolated BCTs was suggested to result from the release of reserve pool vesicles, due to its sensitivity to increased intraterminal Ca^{2+} buffering (Mennerick & Matthews, 1996; Sakaba *et al.* 1997; von Gersdorff *et al.* 1998). In the present study, both the sustained phase of exocytosis and the slow EPSC component exhibit a lower susceptibility to PPD, which may reflect the 3- to 4-fold larger size of the reserve pool relative to the RRP (von Gersdorff *et al.* 1996; Neves & Lagnado, 1999). The evoked release of large numbers of reserve pool vesicles at selected BC release sites could depend on local differences in Ca^{2+} concentration. The specific functional differences between release sites that give rise to the high degree of variability in the temporal EPSC components remain to be determined.

Comparison of BCT C_m measurements with the charge of evoked EPSCs showed that the size of responses mediated by AMPA/kainate receptors alone, or by AMPA/kainate and NMDA receptors, was linearly related to the amount of exocytosis. A linear relationship between exocytosis and postsynaptic response charge has also been observed at photoreceptor ribbon synapses (in the presence of cyclothiazide to prevent AMPA receptor desensitisation; Thoreson *et al.* 2004; Rabl *et al.* 2005), and at hair cell ribbon synapses with afferent fibres (Li *et al.* 2009). The linear relationship at BC synapses provides evidence in support of the assumption that C_m measurements accurately reflect synaptic vesicle release over the range of stimuli used, which mainly comprised strong depolarisations, suggesting that there is little contribution from extrasynaptic vesicular release or endosomal fusion. The accurate detection of BC exocytosis via postsynaptic responses may enable future studies of BC output to be extended to small physiological stimuli that cannot be resolved by C_m measurements.

The ability of AMPA/kainate receptors to signal the amount of glutamate released during sustained depolarisations and paired-pulse stimuli suggests that receptor desensitisation does not occur to a significant extent at this synapse. AMPA receptor-mediated EPSCs at the rod BC to AII synapse are similarly unaffected by receptor desensitisation (Singer & Diamond, 2006). BC exocytosis in goldfish retina also activates postsynaptic NMDA receptors but, unlike in newt retina (Matsui *et al.* 1998), the detection of sustained exocytosis is not dependent on their activation. As postsynaptic receptors can reliably signal the amount of exocytosis, presynaptic release properties (e.g. the size of vesicle pools and their rates of depletion and replenishment) will be a major determinant of the postsynaptic response to BCT depolarisation. Presynaptic properties are important at photoreceptor synapses, where differences in release kinetics rather than in postsynaptic receptors underlie the faster time-course of cone-driven than rod-driven responses (Rabl *et al.* 2005; Cadetti *et al.* 2005). However, postsynaptic properties are also likely to contribute to functional differences in synaptic transfer between subtypes of retinal neurons. For example, ON and OFF BC to ganglion cell synapses have recently been shown to exhibit differences in NMDA receptor subunit composition and localisation (Sagdullaev *et al.* 2006; Zhang & Diamond, 2009). Future experiments will aim to determine how the presynaptic and postsynaptic properties of synaptic transfer differ at BC synapses with specific amacrine and ganglion cell types, and how this relates to the function of these neurons in retinal processing.

References

Beaumont V, Llobet A & Lagnado L (2005). Expansion of calcium microdomains regulates fast exocytosis at a ribbon synapse. *Proc Natl Acad Sci U S A* **102**, 10700–10705.

Burrone J & Lagnado L (2000). Synaptic depression and the kinetics of exocytosis in retinal bipolar cells. *J Neurosci* **20**, 568–578.

Burrone J, Neves G, Gomis A, Cooke A & Lagnado L (2002). Endogenous calcium buffers regulate fast exocytosis in the synaptic terminal of retinal bipolar cells. *Neuron* **33**, 101–112.

Cadetti L, Tranchina D & Thoreson WB (2005). A comparison of release kinetics and glutamate receptor properties in shaping rod–cone differences in EPSC kinetics in the salamander retina. *J Physiol* **569**, 773–788.

Drummond GB (2009). Reporting ethical matters in *The Journal of Physiology*: standards and advice. *J Physiol* **587**, 713–719.

Heidelberger R, Heinemann C, Neher E & Matthews G (1994). Calcium dependence of the rate of exocytosis in a synaptic terminal. *Nature* **371**, 513–515.

Li GL, Keen E, Andor-Ardo D, Hudspeth AJ & von Gersdorff H (2009). The unitary event underlying multiquantal EPSCs at a hair cell's ribbon synapse. *J Neurosci* **29**, 7558–7568.

Llobet A, Cooke A & Lagnado L (2003). Exocytosis at the ribbon synapse of retinal bipolar cells studied in patches of presynaptic membrane. *J Neurosci* **23**, 2706–2714.

Lukasiewicz PD, Lawrence JE & Valentino TL (1995). Desensitizing glutamate receptors shape excitatory synaptic inputs to tiger salamander retinal ganglion cells. *J Neurosci* **15**, 6189–6199.

Maguire G (1999). Rapid desensitization converts prolonged glutamate release into a transient EPSC at ribbon synapses between retinal bipolar and amacrine cells. *Eur J Neurosci* **11**, 353–362.

Matsui K, Hosoi N & Tachibana M (1998). Excitatory synaptic transmission in the inner retina: paired recordings of bipolar cells and neurons of the ganglion cell layer. *J Neurosci* **18**, 4500–4510.

Mennerick S & Matthews G (1996). Ultrafast exocytosis elicited by calcium current in synaptic terminals of retinal bipolar neurons. *Neuron* **17**, 1241–1249.

Mennerick S & Matthews G (1998). Rapid calcium-current kinetics in synaptic terminals of goldfish retinal bipolar neurons. *Vis Neurosci* **15**, 1051–1056.

Neves G & Lagnado L (1999). The kinetics of exocytosis and endocytosis in the synaptic terminal of goldfish retinal bipolar cells. *J Physiol* **515**, 181–202.

Palmer MJ, Taschenberger H, Hull C, Tremere L & von Gersdorff H (2003). Synaptic activation of presynaptic glutamate transporter currents in nerve terminals. *J Neurosci* **23**, 4831–4841.

Rabl K, Cadetti L & Thoreson WB (2005). Kinetics of exocytosis is faster in cones than in rods. *J Neurosci* **25**, 4633–4640.

Sagdullaev BT, McCall MA & Lukasiewicz PD (2006). Presynaptic inhibition modulates spillover, creating distinct dynamic response ranges of sensory output. *Neuron* **50**, 923–935.

Sakaba T, Tachibana M, Matsui K & Minami N (1997). Two components of transmitter release in retinal bipolar cells: exocytosis and mobilization of synaptic vesicles. *Neurosci Res* **27**, 357–370.

Singer JH & Diamond JS (2003). Sustained Ca^{2+} entry elicits transient postsynaptic currents at a retinal ribbon synapse. *J Neurosci* **23**, 10923–10933.

Singer JH & Diamond JS (2006). Vesicle depletion and synaptic depression at a mammalian ribbon synapse. *J Neurophysiol* **95**, 3191–3198.

Singer JH, Lassova L, Vardi N & Diamond JS (2004). Coordinated multivesicular release at a mammalian ribbon synapse. *Nat Neurosci* **7**, 826–833.

Snellman J, Zenisek D & Nawy S (2009). Switching between transient and sustained signalling at the rod bipolar–AII amacrine cell synapse of the mouse retina. *J Physiol* **587**, 2443–2455.

Sterling P & Matthews G (2005). Structure and function of ribbon synapses. *Trends Neurosci* **28**, 20–29.

Thoreson WB, Rabl K, Townes-Anderson E & Heidelberger R (2004). A highly Ca^{2+}-sensitive pool of vesicles contributes to linearity at the rod photoreceptor ribbon synapse. *Neuron* **42**, 595–605.

Veruki ML, Morkve SH & Hartveit E (2003). Functional properties of spontaneous EPSCs and non-NMDA receptors in rod amacrine (AII) cells in the rat retina. *J Physiol* **549**, 759–774.

von Gersdorff H & Matthews G (1997). Depletion and replenishment of vesicle pools at a ribbon-type synaptic terminal. *J Neurosci* **17**, 1919–1927.

von Gersdorff H, Sakaba T, Berglund K & Tachibana M (1998). Submillisecond kinetics of glutamate release from a sensory synapse. *Neuron* **21**, 1177–1188.

von Gersdorff H, Vardi E, Matthews G & Sterling P (1996). Evidence that vesicles on the synaptic ribbon of retinal bipolar neurons can be rapidly released. *Neuron* **16**, 1221–1227.

Williams SR & Mitchell SJ (2008). Direct measurement of somatic voltage clamp errors in central neurons. *Nat Neurosci* **11**, 790–798.

Yazulla S, Studholme K & Wu JY (1986). Comparative distribution of ^{3}H-GABA uptake and GAD immunoreactivity in goldfish retinal amacrine cells: a double-label analysis. *J Comp Neurol* **244**, 149–162.

Zhang J & Diamond JS (2009). Subunit- and pathway-specific localization of NMDA receptors and scaffolding proteins at ganglion cell synapses in rat retina. *J Neurosci* **29**, 4274–4286.

Author contributions

The author was solely responsible for conception and design of the study, data collection, analysis and interpretation, and writing the article. All experiments were performed at Keele University.

Acknowledgements

Thanks to Drs S. Jones, N. Cooper and M. Evans for critically reading the manuscript. This work was funded by a Medical Research Council (MRC) Career Development Award and an MRC New Investigator Research Grant.